The Effect of Initial Rotational Energy on the Adsorption of CO to the (0001) Face of Crystalline Ice I_h at Hyperthermal Energies

Devon O. Niel Gardner, Ayman Al-Halabi, and Geert-Jan Kroes*

Leiden Institute of Chemistry, Gorlaeus Laboratories, PO Box 9502, 2300 RA, Leiden, The Netherlands

Received: August 26, 2003

The influence of initial rotational energy on the adsorption of CO to the (0001) crystalline ice I_h surface has been predicted using molecular dynamics (MD) simulations. The simulations were carried out at a surface temperature (T_s) of 150 K for $J = 0-50$ and incidence energies (E_i) of 24.1, 48.2, and 96.5 kJ mol^{-1}, at normal incidence. Predictions were made for both the trapping probabilities (P_{ads}) and the adsorption lifetimes, τ. At low incidence energies (viz. 24.1 and 48.2 kJ mol^{-1}), there is an approximately exponential decrease in the trapping probability with increased initial rotation; a similar trend is obtained for the adsorption lifetime. At these incidence energies, rotationally mediated adsorption, trapping promoted by energy transfer from motion toward the surface to rotation, acts in tandem with energy transferred to surface vibrations to enhance the adsorption of CO. At higher incidence energies (96.5 kJ mol^{-1}), the trapping probability decreases much less with increasing initial rotational-energy of the CO molecule than at lower E_i. A surprising finding of this work is that the trapping of CO to the ice surface is much more hindered by putting rotational energy into the molecule than it is by putting an equivalent amount of energy into motion toward the surface, even though it is the latter mode from which energy has to flow for trapping to occur. To our knowledge, this is the first system for which this phenomenon has been reported.

1. Introduction

Chemical reactions on water ice surfaces have attracted interest for several years because of their importance in astrochemistry[1−6] and in atmospheric chemistry.[7−11] Ice surfaces can facilitate heterogeneous reactions by trapping molecules on time scales long enough for them to react and form products or by allowing one of the reacting particles to dissociate into ions. Consequently, ice surfaces can alter the gas-phase concentration of many common molecules.

An important example of the role played by chemical reactions on water ice surfaces in environmental chemistry is highlighted by the seasonal depletion of ozone in the stratosphere over the Antarctic region.[7] The inactive reservoir molecules HCl and $ClONO_2$ are converted to Cl_2 (and possibly HOCl) on stratospheric ice particles.[8] These species are photolyzed by UV radiation when sunlight returns to the region in the spring and the Cl radicals that are subsequently produced attack ozone.[7,8] With regards to astrochemistry, molecular "ices", commonly containing H_2O and CO, are thought to be prevalent on the surfaces of nanoscale grains.[4] The influence of these icy grains as a sink for gas phase molecules and as a chemical factory for larger, and sometimes more complex, species directly affects the gas-phase chemistry in star forming regions.

The sticking of CO (the second most abundant molecule in the interstellar medium, ISM) to ice is relevant to the formation of larger molecules in the ISM. Experiments have demonstrated that CO can be converted into CO_2, H_2CO, and CH_3OH.[5,12−14] In the ISM, CO_2 has very low-abundance in the gas-phase and is found mainly in the solid phase.[15] This suggests that CO_2 molecules are formed in chemical reactions on or in the ice surface. Consequently, it becomes clear that the rate of CO_2 and CH_3OH formation depends on the trapping probability, P_{ads}, of CO to the ice surface and on the physisorption lifetime, τ, of the adsorbed CO molecule.

The importance of the CO−ice system may be elicited from detailed studies performed. Experimentally, the interaction of CO with water ice surfaces has been studied primarily by infrared (IR) spectroscopy[16−18] and by measuring adsorption isotherms.[19−21] A CO-ice binding energy of ca. 11.4 kJ mol^{-1} was derived by studying adsorption isotherms.[19,20] Molecular beam techniques have been used to study the scattering of CO [22] from an ice surface, and also to study the scattering of other molecules (N_2 [23] and HCl [24]) and atoms (He [25,26] and Ar [27]) from ice surfaces.

Theoretical studies on the interaction of molecules with ice surfaces have been carried out using ab initio calculations[19−21,28,29] to find the adsorption sites and interaction energies, or with molecular dynamics (MD) methods[27−35] to elicit such information as trapping probabilities. The ab initio calculations of Allouche et al. confirmed that CO absorbs preferentially above dangling surface OH groups through direct interaction with the C atom or the O atom (the latter being slightly less stable)[19,21] Manca et al. predicted that the binding energy of CO to ice is 10−12 kJ mol^{-1}, [21] and this agrees well with the experimental value of 11.4 kJ mol^{-1}.[19] These results were later reproduced in MD simulations using ab initio CO−H_2O pair potentials.[28,29] Molecular dynamics simulations have been performed for Ar [27,33] and H [34] atoms , and for CO [28,29] and HCl [30−32,35] on ice.

Al-Halabi et al.[28,29] performed classical trajectory calculations on the trapping probability, P_{ads} of initially rotationless ($J = 0$) CO on the (0001) surface of crystalline ice I_h (at $T_s = 150$ K), for different incidence energies, E_i and incidence angles, θ_i. It was found that P_s decreased exponentially with E_i and also

* To whom correspondence should be addressed. Tel.: +31-71-527-4396. Fax: +31-71-527-4488. E-mail: g.j.kroes@chem.leidenuniv.nl.

10.1021/jp031013c CCC: $27.50
Published on Web 02/24/2004

decreased with θ_i for $\theta_i > 20°$. In this paper, we investigate the influence of putting initial rotational energy in the CO molecule on the trapping probability and adsorption lifetime of CO adsorbed to ice for different incidence energies, to complement the earlier studies[28,29] Some questions that we address are as follows: Does the trapping probability (and lifetime) decrease systematically with E_{rot} as it does for E_i? Does the trapping probability obey total energy ($E_i + E_{rot}$) scaling, or does it depend in different ways on the E_i and/or E_{rot}?

To understand the trapping of molecules to a surface, a detailed understanding of the energy loss mechanisms available in the gas−surface encounter is essential. Trapping may occur due to loss of translational energy perpendicular to the surface on impact to such modes as (1) surface phonons,[36] (2) translation parallel to the surface,[37] and (3) rotation of the colliding molecule.[38] Time-of-flight experiments and MD simulations on the adsorption of alkanes on Pt(111), Pt(110), and LiF(001) surfaces,[39−42] suggest that initial trapping probabilities are determined to within approximately 10% by the fate of the colliding molecule on the "first bounce".

In elongated molecules such as ethane and propane, rotational excitation serves as an effective temporary energy storage mechanism that facilitates trapping.[39,41,42] Rotational excitation of the molecule at the surface may lead to temporary trapping in the molecule−surface potential well; this process has also been called rotationally mediated selective adsorption (RMSA) and was first observed in scattering of HD from Pt(111).[38] Al-Halabi et al. showed in their study of ($J = 0$) CO adsorption to ice that at hyperthermal E_i the transfer of perpendicular translation energy to the surface is very efficient; approximately 90% of this energy is transferred to the surface within 0.5−1.0 ps.[28,29] Studying the excitation/de-excitation of CO rotation at the ice surface is expected to give some insight into the relative importance of the energy transfer mechanisms that contribute to the trapping of CO on ice.

This paper is structured as follows: In the following section, we present the MD method used to simulate the CO-ice system and the computational tools used in our analysis of the results. The results are presented and discussed in section 3, in which trends are identified and explained. Conclusions are offered in the last section, section 4.

2. Experimental Section

To simulate the adsorption of CO to ice I_h, classical trajectory calculations were performed. The approach used here has been previously applied to the scattering of HCl,[30−32,35] H-atoms,[34] and CO[28,29] from ice I_h.

The ice surface was simulated using the MD method.[43] The surface was modeled using a box with four bilayers of moving water molecules, which were treated as rigid rotors but were otherwise allowed to move according to Newton's equations of motion. These mobile layers were superimposed on two bilayers of fixed water molecules. Each bilayer in this MD surface contained 60 water molecules; this gave a box of 360 water molecules, 240 of which were mobile. To mimic an infinite surface, periodic boundary conditions were applied in the directions parallel to the surface (x and y directions). The MD box had replicated dimensions $x = 22.53$ Å and $y = 23.23$ Å; the thickness of the slab was 21.5 Å. The TIP4P potential[44] was used to define the forces acting between the H_2O molecules because it yields a stable ice I_h structure at the temperature relevant to this study. The initial configuration of the ice surface obeyed the "ice rules", with zero dipole moment.[45] Full details of this ice surface model may be found in ref 46. The surface was equilibrated to a surface temperature (T_s) of 150 K using a computational analogue of a thermostat.[47]

The interaction potential between the CO and H_2O molecules used in these calculations is the same pair potential as described by Al-Halabi et al.[28,29] The interaction was represented as a sum of CO−H_2O pair potentials

$$V_{CO-H_2O} = V_{els} + V_{rep} + V_{disp} \quad (1)$$

where V_{els} represents the electrostatic interaction between the two molecules, V_{rep} the short-range repulsive energy, and V_{dis} the dispersion energy. Details on the exact form of the various terms are available in refs 28 and 29.

In the CT calculations, the H_2O-H_2O and H_2O−CO interactions were set to 0 at long distances (≥10 Å) via the use of a switching function. The Monte Carlo technique[43] was used to select at random the initial orientation of CO, the initial orientation of the rotation angular momentum **J** (which was constrained to be perpendicular to the molecular axis), and the impact position of CO on the ice surface. Calculations were performed at $T_s = 150$ K for $E_i = 24.1$, 48.2 and 96.5 kJ mol^{-1} at normal incidence. The initial angular momentum of CO was selected for rotational states of $J = 0$, 2, 6, 10, 14, 16, 25, and 50 (i.e., $E_{rot} \approx 0$, 0.14, 0.97, 2.5, 4.8, 6.3, 15, and 59 kJ mol^{-1}, respectively). For a given set of conditions, 400 trajectories were run using a time step of ≈ 0.1 fs. The CO molecule was initially located 11.3 Å above the basal plane of the thermalized ice surface, and trajectories were propagated until either the CO−ice distance was again larger than 11.3 Å after reflection from the surface or the integration time was longer than 40 ps. To simulate the collision dynamics, Newton's equations of motion of the impinging CO molecule and the water molecules were integrated using an improved leapfrog algorithm.[48] The CO molecule was treated as a rigid rotor.

Trapping was defined to have occurred for those trajectories exhibiting more than one inner turning point in the z-coordinate of CO for motion normal to the ice surface such that, at the end of the trajectory: (i) The total (potential+kinetic) energy of CO trapped at the surface was below $-kT_s$. (ii) The maximum distance of CO to the surface was 4 Å, the ice surface being operationally defined to be at a height $z = 22.5$ Å (the upward pointing hydrogen atoms are at $z \approx 22.7$ Å, the oxygen atoms are at $z \approx 21.7$ Å in the first monolayer).

Figure 1 shows typical trajectories of CO (a) backscattered into the gas phase without trapping, (b) trapped with eventual desorption into the gas-phase, and (c) trapped without observed desorption during the simulation time. The CO molecules trapped on the ice surface (Figure 1, parts b and c) may be regarded as "CO−ice physisorbed complexes".

The trapping probability, P_{ads} is defined as the number of the trapped trajectories, n, divided by the total number of trajectories, n_o. Consequently, P_{ads} and its estimated error, ΔP_{ads}, may be written as

$$P_{ads} = \frac{n}{n_o} \quad (2)$$

and

$$\Delta P_{ads} = \sqrt{\frac{P_{ads}(1 - P_{ads})}{n_o}} \quad (3)$$

respectively.

The adsorption lifetime τ of CO on ice was calculated using the maximum-likelihood method. For practical purposes, the

trajectories cannot be integrated indefinitely, and the exact lifetimes are known for only a portion of the individual cases under study; consequently, we used the Type I ("time") censored maximum-likelihood method.[49] In the relevant expression, τ is given by the maximum likelihood estimation, $\hat{\theta}$, of the time elapsed between the first and last inner turning point in the *z*-coordinate of CO

$$\tau = \hat{\theta} = \frac{\sum_{i=1}^{r} t_i}{r} + (n-r)\frac{t_c}{r} + t_d \qquad (4)$$

In our simulations, the CO−water complex was observed to exist for a minimum threshold time t_d; the existence of such a threshold time arises because the adsorbed molecule has to complete at least one molecule−surface vibration before it can desorb. In our calculation of the adsorption lifetime τ, the parameter t_d was simply taken equal to the minimum observed adsorption time (∼1 ps). Some complexes, such as that exemplified by Figure 1b, were observed to desorb before the end of the maximum simulation time (40 ps), and the adsorption time associated with such trajectories (the time elapsed between the initial and final turning points) is taken equal to $t_i + t_d$. Time censoring was applied to those complexes for which dissociation was not observed (Figure 1c), and t_c is the censoring time, which is calculated by taking the averaged differences between the first and last turning points of the censored trajectories and subtracting t_d. Furthermore, n is the total number of CO−water complexes formed (number of trapped trajectories) in a given simulation, and r is the number of complexes dissociated before the total simulation time (40 ps). With the parameters defined, the probability that CO is first adsorbed and then desorbs within the maximum simulation time is given by r/n_0.

The error in the lifetime is found from a confidence procedure based on the maximum-likelihood estimate (MLE) of the mean adsorption time $\hat{\theta}$ associated with the distribution of lifetimes θ. In calculating the confidence interval, we take the suggestion (often attributed to Cox[50]) to treat $2r\hat{\theta}/\theta$ as being $\sim \chi^2_{(2r+1)}$,[49] and consequently define

$$\tilde{T} = 2r\hat{\theta} = 2r\tau \qquad (5)$$

To obtain an equitailed, two-sided confidence interval for the average lifetime $\hat{\theta}$, we used

$$\frac{\tilde{T}}{\chi^2_{(2r+1),\alpha/2}} \le \theta \le \frac{\tilde{T}}{\chi^2_{(2r+1),1-\alpha/2}} \qquad (6)$$

where $\alpha = 0.20$ for a 80% confidence interval, which is deemed reasonable for our data set.[51] In our calculations, 400 trajectories were propagated for 40 ps for each set of simulations, which is a large enough number to ensure accurate values of the adsorption probability and lifetime. The use of χ^2 distribution tables[52] allows the subsequent computation of the final confidence interval of θ. The size of the ratio of the confidence interval and the adsorption lifetime, which determines how accurate the lifetime estimate is, depends on both the number of adsorbing trajectories in the batch (i.e., on the number of "lifetime tests") and the ratio of the adsorption time and the censoring time (or total simulation time). Generally, the more trajectories are run, and the larger the censoring time is relative to the adsorption lifetime, the more accurate the calculated average lifetime is. It is possible to accurately determine average lifetimes with the maximum likelihood method also in the situation that the censoring time is smaller than the average lifetime, provided that enough adsorbed trajectories are simulated (and provided that the CO−ice complexes indeed decay via the exponential distribution, which assumption underlies our work). With the number of trajectories we ran, the average lifetimes determined were always at least a factor of 3 larger than the associated double-sided 80% confidence intervals.

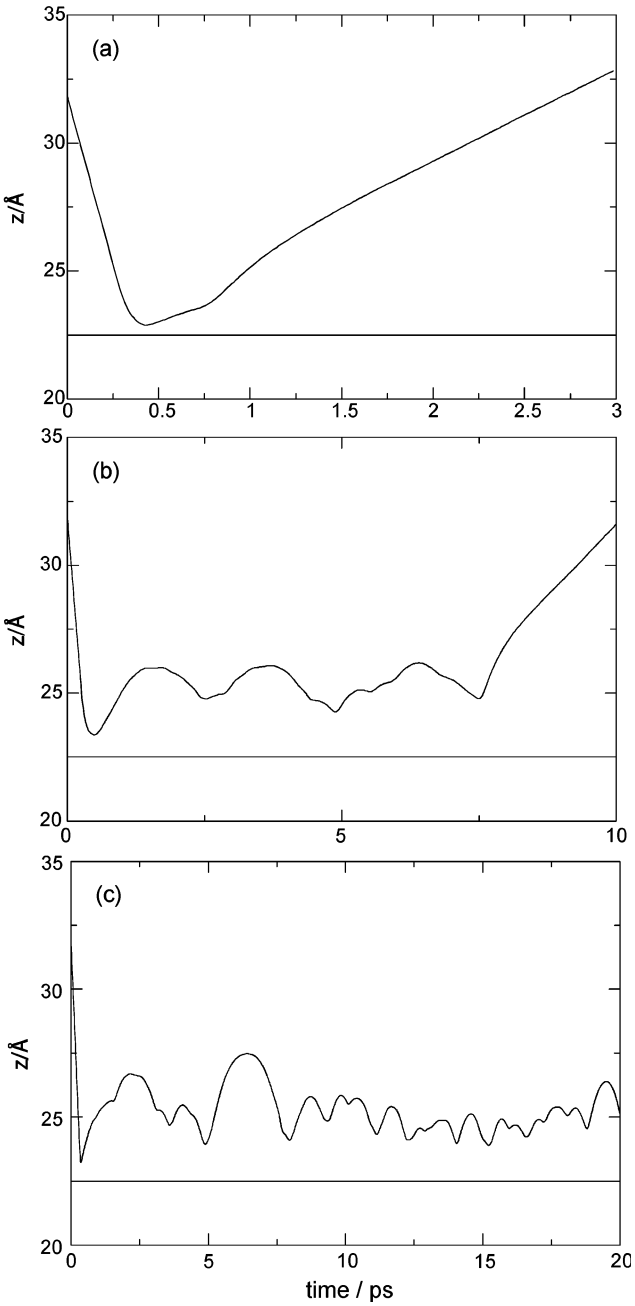

Figure 1. Typical trajectories of CO (**a**) backscattered into the gas phase without trapping, (**b**) trapped with eventual desorption into the gas-phase and (*c*) trapped without observed desorption during the simulation time are shown. The horizontal line at 22.5 Å, in each case, highlights the height of the ice surface, and *z* is the center of mass coordinate of CO for motion perpendicular to the surface.

3. Results and Discussion

The influence of initial rotational energy on the adsorption of CO to the (0001) surface of ice I_h was studied for three incidence energies (24.1, 48.2, and 96.5 kJ mol^{-1}); the results

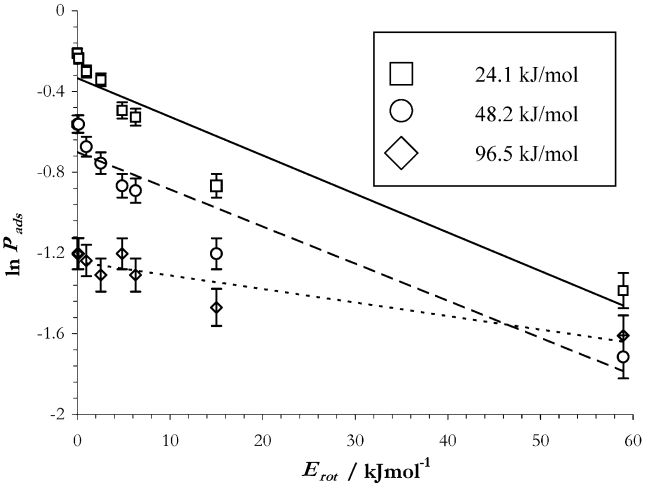

Figure 2. The influence of initial rotational energy on the trapping probability of CO on the (0001) surface of ice I_h is shown for three incidence energies (24.1, 48.2, and 96.5 kJ mol^{-1}), through a plot of ln P_{ads} against E_{rot}. The best-fit lines obtained by nonweighted least-squares fitting are also shown, using a solid line for 24.1 kJ mol^{-1}, a dashed line for 48.2 kJ mol^{-1}, and a dotted line for 96.5 kJ mol^{-1}.

TABLE 1: The Coefficients *a* and *b* Describing the Dependence of the Adsorption Probability on the Rotational Energy Are Given for Three Incidence Energies (eq 7)[a]

E_i (kJ/mol)	a	b (kJ^{-1}mol)	c (kJ^{-1}mol)
24.1	0.716	0.0191	0.0138
48.2	0.497	0.0185	0.0145
96.5	0.288	0.0067	0.0129

[a] The coefficient c (see eq 8a) which fits the adsorption probability given the different b-values for each incidence energy is also given.

are summarized in Figure 2. For the three collision energies studied, ln P_{ads} may be fitted reasonably well to E_{rot}, showing that the trapping probability decreases approximately exponentially with increasing rotational energy. For the expression

$$P_{ads} = a \exp(-bE_{rot}), \tag{7}$$

the fitting coefficients we obtained for the three collision energies are listed in Table 1. As can be seen from Figure 2, especially for $E_i = 24.1$ and 48.2 kJ/mol, the data are above the fitted line for low and high rotational energies and below it for intermediate energies. This suggests that a biexponential dependence would result in an improved fit. We have not pursued this further because the main physical trends are emphasized more through the monoexponential fits.

If the dependence on the incidence energy is approximately incorporated by replacing a with $\exp(-cE_i)$, we obtain

$$P_{ads} = \exp(-bE_{rot} - cE_i) \tag{8a}$$

The c-coefficients are likewise collected in Table 1. For low E_i ($\leq$ 48.2 kJ mol^{-1}), we find that

$$P_{ads} \approx \exp(-0.019E_{rot} - 0.014E_i), \tag{8b}$$

the E_i-dependence of which is similar to the previously obtained expression $P_{ads} \approx 0.9 \exp(-0.012E_i)$ obtained by Al-Halabi et. al for ($J = 0$) CO.[28,29] The fact that the E_{rot} coefficient, b, is larger than the E_i coefficient, c (eqs 8a and 8b), at these energies (see Table 1) shows surprisingly that the trapping of CO is more strongly hindered by putting rotational energy into the molecule than it is by putting a similar quantity of energy into the motion toward the surface, as is also apparent from Figure 2. Equation

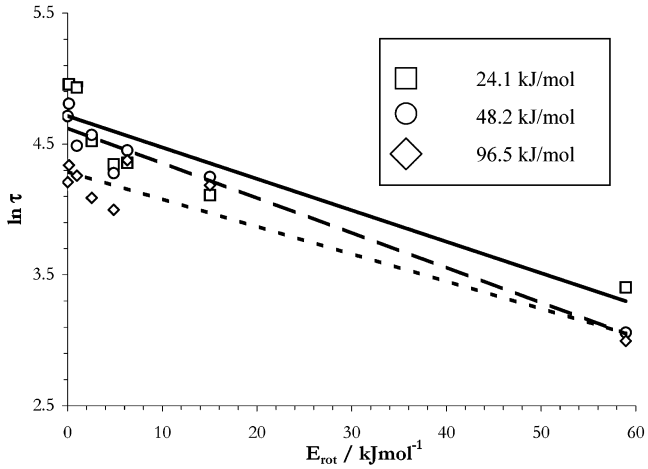

Figure 3. The influence of initial rotational energy on the adsorption lifetime of CO on the (0001) surface of ice I_h is shown for three incidence energies (24.1, 48.2, and 96.5 kJ mol^{-1}), through a plot of ln τ (where τ is in ps) against E_{rot}. The best-fit lines obtained by nonweighted least-squares fitting are also shown, using a solid line for 24.1 kJ mol^{-1}, a dashed line for 48.2 kJ mol^{-1}, and a dotted line for 96.5 kJ mol^{-1}.

TABLE 2: The Coefficients *d* and *f* Describing the Dependence of the Adsorption Lifetime on the Rotational Energy Are Given for Three Incidence Energies (eq 10)

E_i (kJ/mol)	d(ps)	f (kJ^{-1}mol))
24.1	110	0.024
48.2	102	0.026
96.5	73	0.021

8b does not apply to higher E_i: For $E_i = 96.5$ kJ mol^{-1}, P_{ads} falls off much more slowly with increasing rotational energy than it does for $E_i = 24.1$ and 48.2 kJ mol^{-1}. The breakdown of this relationship is not due to the effect of translational energy; as found before,[28,29] P_{ads} for ($J = 0$) CO can be fitted quite well to an exponentially decaying function of E_i, for $E_i = 9.6-187$ kJ mol^{-1}.

The influence of initial rotational energy on the lifetime of CO adsorbed to the ice I_h surface was studied for the same incidence energies (see Figure 3). The computed lifetimes all fall in the range of 20−140 ps. There is an approximately linear dependence of ln τ on E_{rot} (Figure 3), suggesting that the adsorption lifetime also decreases approximately exponentially with increasing rotational energy

$$\tau = d \exp(-fE_{rot}) \tag{9}$$

The fitting coefficients we obtained for the three collision energie are listed in Table 2. As was the case for P_{ads}, the relationship between τ and E_{rot} is very similar for 24.1 and 48.2 kJ mol^{-1}, but different for 96.5 kJ mol^{-1}; τ is suppressed more strongly by E_{rot} at low E_i ($\leq$48.2 kJ mol^{-1}) than at higher E_i ($E_i = 96.5$ kJ mol^{-1}).

The trapping probability and adsorption lifetime are plotted in Figure 4 as a function of the total (translational + rotational) initial energy E_{tot} of CO to further highlight the individual roles of E_{rot} and E_i in the adsorption process. The main purpose of this was to illustrate that these quantities do not obey total energy scaling. Molecules with a similar total energy but with low initial rotational energy and high initial translational energy show a much higher adsorption probability than molecules with high initial rotational energy but low initial translational energy. This result for P_{ads} could have been anticipated for low E_i (24.1 and 48.2 kJ mol^{-1}), for which we found that $P_{ads} \approx \exp(-0.019E_{rot}$

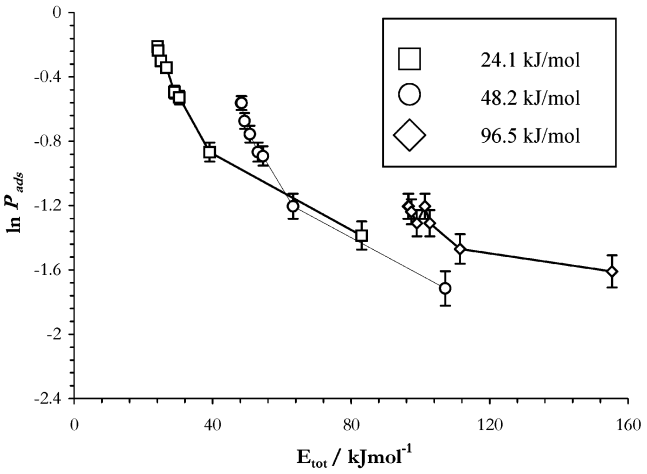

Figure 4. The dependence of ln P_{ads} on E_{tot}. ($=E_{rot} + E_i$) is shown for three sets of data, each of which corresponds to a specific incidence energy (24.1, 48.2, and 96.5 kJ mol^{-1}). Data for a specific incidence energy are connected by lines, to guide the eye.

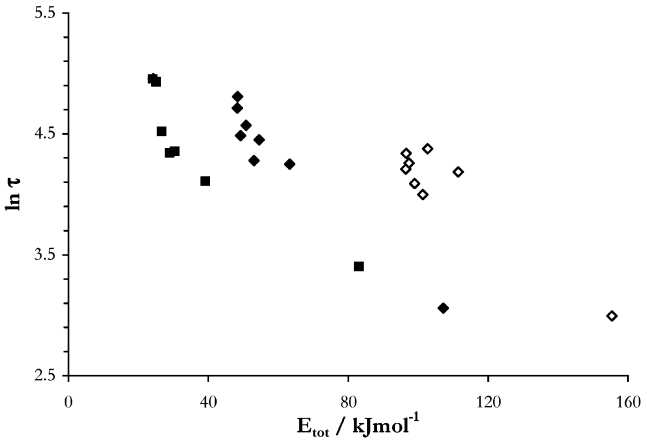

Figure 5. The dependence of ln τ on E_{tot}. ($=E_{rot} + E_i$) is shown. The points for the various incidence energies are marked by filled squares for $E_i = 24.1$ kJ mol^{-1}, filled diamonds for $E_i = 48.2$ kJ mol^{-1}, and open diamonds for $E_i = 96.5$ kJ mol^{-1}.

$- 0.014E_i$), with the coefficient for E_{rot} being larger than that of E_i (eq 8b). Plotting ln τ against E_{tot} (**Figure 5**) shows the same trend for the adsorption lifetime. There are large disparities between P_{ads} and τ for total energies within the same regime but with different contributions of E_i and E_{rot}.

Although each trajectory is unique, many single trajectories do exhibit some common characteristics, and individual trajectories can therefore be helpful in providing insights into the collision dynamics. Figures 6 and 7 show how rotational excitation may result in the trapping of ($J = 0$) CO even at $E_i = 96.5$ kJ mol^{-1}. In the trajectory of Figure 6, there is a clear enhancement of rotation on the "first bounce" and an accompanying efficient transfer of incidence energy. More than 10 kJ mol^{-1} of the incidence energy (which is more than the average binding energy to the surface) is transferred to rotation upon "first bounce", and together with the energy transferred to the surface phonons, this is sufficient to trap CO. In **Figure 7** (a typical scattering trajectory), there is no significant rotational excitation on the "first bounce", and the molecule is scattered directly with approximately 12 kJ mol^{-1} of translational energy remaining in the molecule.

Because collisions generally have the effect of moving a system closer toward energy partitioning, it is easier to rotationally excite initially nonrotating or slow-rotating molecules

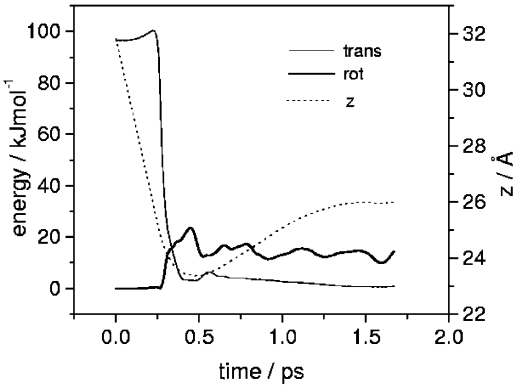

Figure 6. A typical adsorbed trajectory showing rotational excitation accompanied by trapping upon collision of CO with the ice surface. The translational energy (thin solid line) and rotational energy (thick solid line) are shown as a function of time (energy-axis on the left). The height of the ice surface was operationally defined to be at 22.5 Å, and the dotted line shows the *z*-coordinate of CO as a function of time (*z*-axis on the right). The "first bounce" is at the first turning point in the *z*-coordinate.

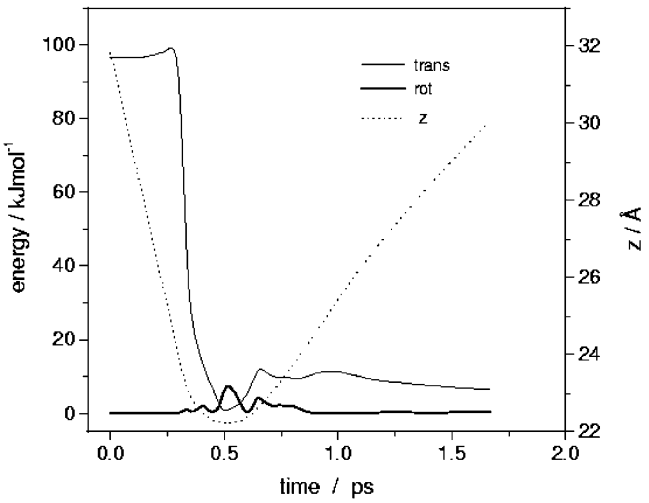

Figure 7. A typical scattering trajectory showing only little rotational excitation of CO upon collision with the ice surface. The transfer of incidence energy (thin solid line) to rotational energy (thick solid line) is not as efficient as that in the case of the adsorbed trajectory. All other definitions are as in the previous figure.

than fast-rotating molecules. Consequently, the probability of rotational excitation is larger for initially nonrotating or slow-rotating CO than fast-rotating CO. The depression of this mode of energy storage (rotational excitation) explains the concomitant decrease in trapping probability with increasing rotational energy for all three incidence energies studied (Figure 2). The observed decrease in adsorption lifetime with increasing rotational energy (Figure 3) is also consistent with this model. On bounces after the initial collision, the rotational energy of initially rotating CO can be converted to normal kinetic energy, which can result in the desorption of CO from the ice surface. Usually, initially fast-rotating CO will have a higher rotational energy than initially nonrotating or slow-rotating CO after the "first bounce", and consequently, chattering is likely to occur and cause it to desorb more quickly from the surface.

Further proof of the role played by rotational excitation in the trapping of CO to the ice I_h surface is given in Figure 8. In these plots, the average of ΔE_{rot} (the difference between the initial rotational energy and the rotational energy after the "first bounce") was determined for trapped and backscattered trajectories at $E_i = 48.2$ kJ mol^{-1}. In adsorbed trajectories, rotational

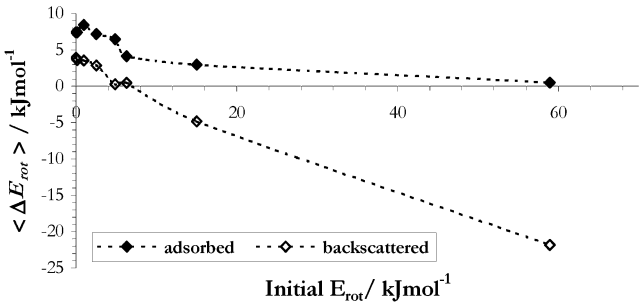

Figure 8. The average change in rotational energy for adsorbed and backscattered CO is shown for various initial rotational energies at $E_i = 48.2$ kJ mol^{-1}. This highlights the role of rotational excitation in trapping; on average, adsorbed molecules are rotationally excited. Rotational excitation decreases with increasing E_{rot}. See text for explanations.

excitation, resulting in energy transfer to rotation of 5 kJ mol^{-1} or more for $J \leq 16$ ($E_{rot} \leq 6.5$ kJ mol^{-1}), contributed to the trapping of CO at the ice surface. This is consistent with the picture garnered from Figure 6 and findings for molecules such as ethane and propane, in which rotational excitation serves as an effective temporary energy storage mechanism that facilitates trapping.[39,41,42] Even at higher rotational states ($J > 16$), there was no net transfer of energy away from rotation. Conversely, backscattered trajectories showed very little enhancement of rotational energy for $J \leq 16$ and loss of rotational energy for higher rotational states ($J > 16$). Thus, at high j it is not just that it becomes less likely that CO is rotationally excited. Instead, on average, CO loses rotational energy to either the surface or the CO translational motion, which would directly lead to a decrease in the trapping probability in the latter case.

As we saw, the depression of energy storage in rotations with increased initial rotation of CO provided at least a partial explanation for the inhibition of trapping by initial rotation. However, the transfer of rotational energy to the phonons (the motions of the surface water molecules) should also be considered. The importance of energy transfer to the surface is underlined by the fact that in previous calculations on adsorption of initially nonrotating ($J = 0$) CO to ice we found that most of the translational energy of CO is lost to the surface H_2O molecules and not to the CO rotation (refs 28 and 29); this is also illustrated for a typical trajectory in Figure 6, where only a small part of the initial translational energy is seen to flow to rotation. Now, as previously mentioned, the trapping of CO to the ice surface is much more hindered by putting rotational energy into the molecule than it is by putting an equivalent amount of energy in translation normal to the surface. This is a surprising result, given that, for trapping to occur, the molecule has to transfer its translation energy normal to the surface to other modes. The result suggests that in the CO-ice system, the translation normal to the surface is more strongly coupled to the surface phonons than the molecule's rotation, so that the molecule's normal translational energy is more efficiently transferred to the surface. The molecule's rotations are most strongly coupled to the translation normal to the surface, and this coupling becomes active when the molecule is close to the surface. This allows rotational energy to flow to translational motion normal to the surface on the first bounce; a point of time in the trajectory where the molecule is close to its first turning point in z and is "making up its mind" on whether to be trapped or backscattered. This can explain why rotational energy is so efficient at inhibiting trapping: The molecule's rotations are not strongly coupled to the surface, but through the interaction with the surface, they are strongly coupled to the molecule's translation at a point in the trajectory where energy transfer to translation is likely to result in desorption. The weak coupling of the rotations with the surface motions also provide an additional explanation for the inhibition of trapping by initial rotation: due to this weak coupling, initial rotational energy is more likely to flow to the translational motion of CO on the first bounce, which will promote direct scattering and inhibit trapping.

Molecular adsorption requires dissipation of the incident energy, ultimately leading to thermal accommodation with the surface. At $E_i = 96.5$ kJ mol^{-1}, the dissipation required for adsorption at this surface is very large and so trapping at this energy is already a low probability event even for initially nonrotating CO; $P_{ads} \approx 0.3$ for ($J = 0$) CO. Suppression of P_{ads} and/or τ by initial rotation, to a similar degree as observed for the lower incidence energies (24.1 and 48.2 kJ mol^{-1}), is unlikely due to energy partitioning; at $E_i \geq 96.5$ kJ mol^{-1}, less energy will flow from rotation to perpendicular translational energy than at 24.1 and 48.2 kJ mol^{-1}, because there is already so much energy present in translation.

We have also looked at the effect of impact site on the trapping probability. In previous calculations on scattering of HCl from ice, we found that HCl could penetrate the surface at the highest energy considered here (96.5 kJ/mol) in collisions in which HCl impacts near the center of a surface hexagon ring.[31,32] Interestingly, such collisions of CO with the ice surface do not lead to penetration, but they may lead to surface damage.[28,29] However, we did not find any indication that the adsorption probability depends on the impact site. Due to the favorable ratio of the mass of the collider (CO) and of the collision center (1−6 molecules), adsorption is efficient at low energies regardless of impact site.[28,29]

In principle, it is possible to compute the adsorption lifetimes τ of CO to the ice surface by integrating out all the adsorbed trajectories until the molecule desorbs from the surface; τ can then be found by taking the average of the computed trapping times. Usually, however, τ is much larger than the time over which the trajectories can be practically propagated (∼40 ps). To calculate τ, we used the "time"-censored maximum-likelihood method (eq 4).[49] An alternate method, which requires only an estimate of the adsorption energy and the molecule−surface vibrational frequency and is used generally in astrochemical models,[53,54] is the statistical mechanics model of Frenkel.[55] If the assumptions are made that (i) the trapping probability is close to 1.0, (ii) the surface coverage is low, (iii) the CO−ice potential is dependent only on the z-coordinate (the distance of CO to the ice surface), and (iv) the vibration of the molecule in the surface potential well is harmonic, then the lifetime from the Frenkel model, τ_F can be calculated from[30]

$$\tau_F = \tau_v \exp\left(\frac{u}{kT_s}\right). \quad (10)$$

In eq 10, τ_v is the vibrational period of the molecule on the surface (which is obtainable from the number of turning points in z for adsorbed trajectories), $u = E_b + (1/2)kT_s$; E_b is the average binding energy of the molecule to the surface (which is taken as a positive number), and k is the Boltzmann constant. The Frenkel model represents a rather crude way of estimating the adsorption lifetime, which can however be applied in situations where the adsorption lifetime exceeds the computationally feasible simulation time by more than an order of magnitude, and which, as stated before, is extensively used in astrophysical modeling.[53,54,56−58] In fact, as far as we know, in every gas−grain astrochemical model (i.e., model incorporating

molecule−surface reactions) eq 10 is used to model the desorption of reactant and product molecules from surfaces, employing estimates of τ_v and u.

We applied the Frenkel model to ($J = 0$) CO adsorbed on ice for $E_i = 24.1$ kJ mol^{-1} to compare its performance with the maximum likelihood method for this system. The average binding energy, E_b was 7.28 kJ mol^{-1}, which gave $u = 7.91$ kJ mol^{-1} ($kT_s = 1.25$ kJ mol^{-1} for $T_s = 150$ K). Additionally, τ_v was computed to be 0.7 ps. Application of eq 10 then gives $\tau_F = 390$ ps. This value agrees with the maximum likelihood lifetime, 141.9 ps, to within a factor e. The Frenkel model is valid for systems at thermodynamic equilibrium, which results most readily for low E_i and low E_{rot}, with $P_{ads} \approx 1$, in classical dynamics, and therefore comparison with results for higher E_i and E_{rot} would not be useful. The maximum likelihood adsorption lifetime was not reproduced by the Frenkel model because in our system there is no immediate thermodynamic equilibrium as assumed by the model: $E_i = 20\ kT_s$. Further, the CO−ice potential depends on molecular coordinates other than z. Nonetheless, the Frenkel model is here seen to provide a reliable order of magnitude estimate of the physisorption lifetime, suggesting that it may be usefully applied in astrochemical models.

4. Conclusions

Results of classical trajectory calculations on the influence of initial rotational energy of hyperthermal CO on its adsorption to the basal plane (0001) face of ice I_h were presented. The results show that the trapping probability and the adsorption lifetime decrease approximately exponentially with increasing rotational energy. Conversely, for low initial rotational energies, adsorption can be assisted by the transfer of incidence energy into rotation of the colliding molecule (rotationally mediated adsorption, RMA), although the dominant energy transfer mechanism responsible for trapping is energy transfer to the ice surface.

At low incidence energies ($E_i = 24.1$ and 48.2 kJ mol^{-1}), the addition of rotational energy to ($J = 0$) CO surprisingly suppresses trapping much more than does the addition of a similar quantity of energy to motion toward the surface (i.e., the mode from which energy should be removed for trapping to occur). This suggests that for the CO−ice system, the molecule's translation normal to the surface is much more strongly coupled to the surface phonons than is the molecule's rotation. Because the molecule's rotation is strongly coupled to its translation normal to the surface when the molecule is close to the surface, energy can flow from rotation to translational motion normal to the surface close to the inner turning point of the trajectory, thereby promoting desorption.

The adsorption lifetime obtained with the Frenkel method (a statistical mechanical method only requiring estimates of the adsorption energy and the molecule−surface vibrational frequency) was compared with that obtained using the more exact maximum likelihood method in which the lifetime was obtained by running dynamics calculations. The lifetime obtained with the Frenkel model agreed with the more exact value to within a factor e, suggesting that the Frenkel method can be usefully applied to astrochemical models, which often only require order of magnitude estimates of physisorption lifetimes.

Acknowledgment. This project was supported by the Nederlandse Organisatie voor Wetenschappelijk Onderzoek (NWO) through a CW-program grant and by a grant of computer time from the National Computing Facilities Foundation (NCF). We are grateful to Professor Gianluigi Boca for useful suggestions on the error analysis of the maximum-likelihood adsorption lifetimes.

References and Notes

(1) Ehrenfreund, P.; Schutte, W. A. Astrochemistry : from molecular clouds to planetary systems : proceedings of the 197th symposium of the International Astronomical Union held in Sogwipo, Cheju, Korea, 23-27 August 1999; Minh, Y. C., Van Dishoeck, E. R., Eds.; Astronomical Society of the Pacific: San Francisco, CA 2000; p 135.

(2) Tielens, A. G. G. M.; Tokunaga, A. T.; Geballe, T. R.; Baas, F. *Astrophys. J.* **1991**, *381*, 181.

(3) Tanaka, M.; Nagata, T.; Sato, S.; Yamamoto, T. *Astrophys. J.* **1994**, *430*, 779.

(4) Allamandola, L. J.; Bernstein, M. P.; Sandford, S. A.; Walker, R. L. *Space Sci. Rev.* **1999**, *90*, 219.

(5) Hudson, R. L.; Moore, M. H. *Icarus* **1999**, *140*, 451.

(6) Hudson, R. L.; Moore, M. H. *Icarus* **2000**, *145*, 661.

(7) Solomon, S.; Garcia, R. R.; Rowland, F. S.; Wuebbles, D. J. *Nature* **1986**, *321*, 755−758.

(8) Molina, M. J.; Tso, T. L.; Molina, L. T.; Wang, F. C. Y. *Science* **1987**, *238*, 1253.

(9) Molina, M. J. *Angew. Chem., Int. Ed. Engl., Nobel Lecture* **1996**, *35*, 1778.

(10) Rowland, F. S. *Angew. Chem., Int. Ed. Engl., Nobel Lecture* **1996**, *35*, 1786.

(11) Solomon, S. *Geophys.* **1999**, *73*, 275.

(12) Tielens, A. G. G. M.; Hagen, W. *Astron. Astrophys.* **1982**, *114*, 245.

(13) Allamandola, L. J.; Sandford, S. A.; Valero, G. J. *Icarus* **1988**, *76*, 225.

(14) Schutte, W. A.; Gerakines, P. A.; Geballe, T. R.; van Dishoeck, E. F.; Greenberg, J. M. *Astron. Astrophys.* **1996**, *309*, 663.

(15) van Dishoeck, E. F.; Helmich, F. P.; de Graauw, T.; Black, J. H.; Boogert, A. C. A.; Ehrenfreund, P.; Gerakines, P. A.; Lacy, J. H.; Millar, T. J.; Schutte, W. A.; Tielens, A. G. G. M.; Whittet, D. C. B.; Boxhoorn, D. R.; Kester, D. J. M.; Leech, K.; Roelfsema, P. R.; Salama, A.; Vandenbussche, B. *Astron. Astrophys.* **1996**, *315*, L349.

(16) Sandford, S. A.; Allamadola, L. J.; Tielens, A. G. G. M.; Valero, G. J. *Astrophys. J.* **1988**, *329*, 498.

(17) Devlin, J. P. *J. Phys. Chem.* **1992**, *96*, 6185.

(18) Palumbo, M. E. *J. Phys. Chem. A* **1997**, *101*, 4298.

(19) Allouche, A.; Verlaque, P.; Pouricin, J. *J. Phys. Chem. B* **1998**, *102*, 89.

(20) Manca, C.; Roubin, P.; Martin, C. *Chem. Phys. Lett.* **2000**, *330*, 21.

(21) Manca, C.; Martin, C.; Allouche, A.; Roubin, P. *J. Phys. Chem. B* **2001**, *105*, 12861.

(22) Suter, M. T.; Andersson, P. U.; Pettersson, J. B. C. *XXIII ICPEAC: Topical Issue of Physica Scripta*, submitted for publication.

(23) Gotthold, M. P.; Sitz, G. O. *J. Phys. Chem. B* **1998**, *102*, 9557.

(24) Andersson, P. U.; Någård, M. B.; Pettersson, J. B. C. *J. Phys. Chem. B* **2000**, *104*, 1596.

(25) Glebov, A.; Graham, A. P.; Menzel, A.; Toennies, J. P. *J. Chem. Phys.* **1997**, *106*, 9382.

(26) Braun, J.; Glebov, A.; Graham, A. P.; Menzel, A.; Toennies, J. P. *Phys. Rev. Lett.* **1998**, *80*, 2638.

(27) Andersson, P. U.; Någård, M. B.; Bolton, K.; Svanberg, M.; Pettersson, J. B. C. *J. Phys. Chem. A* **2000**, *104*, 2681.

(28) Al-Remawi, A. *Dynamics of Molecules on Ice*, Ph.D. Thesis, Leiden University of Leiden; 2002.

(29) Al-Halabi, A.; Kleyn, A. W.; van Hemert, M. C.; van Dishoeck, E. F.; Kroes, G. J. *J. Phys. Chem. A* **2003**, in print.

(30) Kroes, G. J.; Clary, D. C. *J. Phys. Chem.* **1992**, *96*, 7079.

(31) Al-Halabi, A.; Kleyn, A. W.; Kroes, G. J. *Chem. Phys. Lett.* **1999**, *307*, 505−510.

(32) Al-Halabi, A.; Kleyn, A. W.; Kroes, G. J. *J. Chem. Phys.* **2001**, *115*, 482−491.

(33) Bolton, K.; Pettersson, J. B. C. *Chem. Phys. Lett.* **1999**, *312*, 71.

(34) Al-Halabi, A.; Kleyn, A. W.; van Dishoeck, E. F.; Kroes, G. J. *J. Phys. Chem. B* **2002**, *106*, 6515−6522.

(35) Gardner, D. O. N.; Al-Halabi, A.; Kroes, G. J. *Chem. Phys. Lett.* **2003**, *376*, 581−587.

(36) Evans, D.; Celli, V.; Benedek, G.; Toennies, J. P.; Doak, R. B. *Phys. Rev. Lett.* **1983**, *50*, 1854.

(37) Lennard-Jones, J. E.; Devonshire, A. F. *Nature* **1936**, *137*, 1069.

(38) Cowin, J. P.; Yu, C. F.; Sibener, S. J.; Hurst, J. E. *J. Chem. Phys.* **1981**, *75*, 1033.

(39) Stinnett, J. A.; Madix, R. J.; Tully, J. C. *J. Chem. Phys.* **1996**, *104*, 3134.

(40) Stinnett, J. A.; Madix, R. J. *J. Chem. Phys.* **1996**, *105*, 1610.

(41) Weaver, J. F.; Madix, R. J. *J. Chem. Phys.* **1999**, *110*, 10585.
(42) Tomii, T.; Kondo, T.; Yagyu, S.; Yamamoto, S. *J. Vac. Sci. Technol. A* **2001**, *19*, 675.
(43) Allen, M. P.; Tildesley, D. J. *Computer Simulations of Liquids*; Clarendon: Oxford, 1987.
(44) Jorgensen, W. L.; Chandrasekhar, J.; Madura, J. D.; Impey, R. W.; Klein, M. L. *J. Chem. Phys.* **1983**, *79*, 926.
(45) Bernal, J. D.; Fowler, R. H. *J. Chem. Phys.* **1936**, *1*, 515.
(46) Kroes, G. J. *Surf. Sci.* **1992**, *275*, 365.
(47) Berendsen, H. J. C.; Postma, J. P. M.; van Gunsteren, V. F.; Dinola, A.; Haak, J. R. *J. Chem. Phys.* **1984**, *81*, 3684.
(48) Fincham, D. *Mol. Simul.* **1992**, *8*, 165.
(49) Lawless, J. F., *Statistical Models and Methods for Lifetime Data*; Wiley: New York, 1982.
(50) Cox, D. R. *Biometrika* **1953**, *40*, 353.
(51) Sundberg, R. *Lifetime Data Anal.* **2001**, *7*, 393.
(52) Hays, W. L. *Statistics*; Holt− Saunders: Tokyo, 2001.
(53) Sandford, S. A.; Salema, F.; Allamandola, L. J.; Trafton, L. M.; Lester, D. F.; Ramseyer, T. F. *Icarus* **1991**, *91*, 125.
(54) Sandford, S. A.; Allamandola, L. J. *Astrophys. J.* **1993**, *417*, 815.
(55) Frenkel, J. *Z. Phys.* **1924**, *26*, 117.
(56) Augason, G. C. *Astrophys. J.* **1970**, *162*, 463.
(57) Goodman, F. O. *Astrophys. J.* **1978**, *226*, 87.
(58) Pirronello, V.; Biham, O.; Liu, C.; Shen, L. O.; Vidali, G. *Astrophys. J.* **1997**, *483*, L131.